

Automatic Tuned MRI RF Coil for Multinuclear Imaging of Small Animals at 3T

L. Tugan Muftuler, Gultekin Gulsen, Kumsal D. Sezen,¹ and Orhan Nalcioglu

John Tu and Thomas Yuen Center for Functional Onco-Imaging, College of Medicine, University of California, Irvine, California 92697

Received June 21, 2001; revised December 04, 2001

We have developed an MRI RF coil whose tuning can be adjusted automatically between 120 and 128 MHz for sequential spectroscopic imaging of hydrogen and fluorine nuclei at field strength 3 T. Variable capacitance (varactor) diodes were placed on each rung of an eight-leg low-pass birdcage coil to change the tuning frequency of the coil. The diode junction capacitance can be controlled by the amount of applied reverse bias voltage. Impedance matching was also done automatically by another pair of varactor diodes to obtain the maximum SNR at each frequency. The same bias voltage was applied to the tuning varactors on all rungs to avoid perturbations in the coil. A network analyzer was used to monitor matching and tuning of the coil. A Pentium PC controlled the analyzer through the GPIB bus. A code written in LABVIEW was used to communicate with the network analyzer and adjust the bias voltages of the varactors via D/A converters. Serially programmed D/A converter devices were used to apply the bias voltages to the varactors. Isolation amplifiers were used together with RF choke inductors to provide isolation between the RF coil and the DC bias lines. We acquired proton and fluorine images sequentially from a multicompartment phantom using the designed coil. Good matching and tuning were obtained at both resonance frequencies. The tuning and matching of the coil were changed from one resonance frequency to the other within 60 s. © 2002 Elsevier Science (USA)

Key Words: MRI; birdcage coil; automatic tuning; MRI spectroscopy.

INTRODUCTION

Various double tuned RF coil designs have been proposed for multinuclear MR imaging. However, there are several challenges in these designs. For the fixed capacitor birdcage coils, one has to do fine tuning and matching of the coil at both frequencies using variable capacitors attached to several rungs or segments of the end ring, making such manual procedures time consuming. Furthermore, the perturbations caused by the variable capacitors on one or more birdcage elements result in nonuniform B1 distribution inside the coil volume (1). Moreover, in the passive-tuned coils, tuning and matching changes with different loads, causing variability in SNR obtained from different samples.

A popular method for obtaining double-resonant operation of birdcage coils is to split the two degenerate modes by intentionally perturbing the coil on one or more of the segments (2). However, as the frequency difference between the two operating frequencies increases, B1 inhomogeneities become emphasized (3). Therefore, this method can only be used to image nuclei with resonance frequencies close to each other, and preferably at 1.5 T and lower field strengths.

Another proposed method is to use bandpass or bandstop architectures in which one uses extra inductor/capacitor combinations to achieve double-resonant operation (4, 5). But as was already mentioned in an article by Rath (4), it is hard to achieve good matching at both frequencies, and he proposed a readjustment of matching capacitor each time one has to switch between the frequencies.

Vaughan *et al.* proposed and tested a novel RF coil design using the cavity resonator concept for MRI imaging at high frequencies (6). They also showed that it is possible to use this design for dual-frequency operation by tuning odd-numbered rungs to one resonance frequency and even-numbered ones to the other. They achieved high Q and good matching at two frequencies, 70 and 170 MHz. With this concept, it is also possible to tune it to more than two nuclei. However, when the spectrum of the degenerate modes of the two resonant frequencies were observed in the article, it is seen that the modes for each tuning frequency span a bandwidth of roughly 10–12 MHz. Therefore, when this design is used for imaging nuclei such as hydrogen and fluorine, whose resonance frequencies are separated by approximately 8 MHz, higher order modes of one tuning frequency might interfere with the desired mode of the other, resulting in highly inhomogeneous B1 fields. This will bring extra challenges in the implementation. Besides, difficulties in construction and tuning of TEM coils were noted by the author who first proposed the design (7).

A four-ring birdcage structure was designed by Murphy-Boesch *et al.* for H-1 decoupled P-31 spectroscopy of the human head. This design comprises three separate birdcage structures joined together on the same cylindrical surface. The two outer structures resonate at H-1 frequency and the inner structure resonates at P-31 frequency. As described by the authors, this coil also requires tuning for each individual subject. It is reported

¹ Present address: Perkin-Elmer Instruments, Cypress, California.

that tuning for each subject takes about 5–10 mins for a person with an average-sized head. Moreover, it is observed from the spectrum of the full coil that mode 4 of the inner structure is very close to the desired mode 1 of the outer structure. This might cause interference of these two modes if slight perturbations occurred, which would lead to B1 inhomogeneity. Another design challenge is the B1 homogeneity of both coil structures. Inner structure has to be kept short for optimum performance of outer structures; on the other hand, it has to be long enough to get sufficient B1 homogeneity. It is reported that with 125-mm-long inner structure, the sensitivity and transmitter efficiency of the outer structure drop 10–15% compared to a standard two-ring birdcage of the same size.

Several autotuning methods have been proposed in the past for tuning RF coils. Hyde *et al.* proposed a piezoelectric-controlled trimmer capacitor to tune the coil (8). However, they were not trying to deal with coil matching. Moreover, they used it to perform fine tuning at a single frequency by adjusting a single capacitor. Rousseau *et al.* described an automatic tuning of a surface coil using a single varactor controlled by a computer (9). This article again discusses fine tuning of the coil at a single frequency. Another approach based on an electric motor coupled to the trimmer capacitors with hydraulic lines was discussed by Hwang *et al.* (10). This method also describes fine tuning of a coil around a single frequency by adjusting a single capacitor for tuning and another for matching.

In the present work, we propose a new low-pass birdcage coil whose capacitors on all rungs can be adjusted at the same time electronically with a computer-controlled system. This eliminates the need for perturbing the coil or trying to obtain optimum matching and tuning at both frequencies. In order to test our design, we used variable capacitance diodes (Varactor) on all rungs in series with fixed capacitors to sweep the resonance frequency of the coil between the resonance frequencies of hydrogen and fluorine at 3T field strength. We used a separate varactor diode pair for impedance matching. Images were acquired from samples of CuSO_4 and C_6F_6 solutions placed in small tubes using the developed coil.

METHODS

We designed and constructed a low-pass, 8-element transmit–receive birdcage coil for small animal imaging. We chose to use an 8-leg configuration instead of 16 legs for the birdcage design to obtain higher Q, hence a better SNR (5). The coil was 10.75 cm in diameter and 17 cm in length. This was placed inside an RF shield with diameter 295 mm. Two varactor diodes (Knox Semiconductor, Inc., SMV2109) connected cathode-to-cathode and in series with an 18-pF capacitor were used in each rung for tuning. The capacitance of the varactor diodes changed from 70 to 30 pF with an applied reverse bias voltage of 0 to 5 V. The tuning of the operating frequency of the coil was obtained by changing the applied bias voltage on all rungs at the same time, from a single source. To obtain the same capacitance value on each rung of

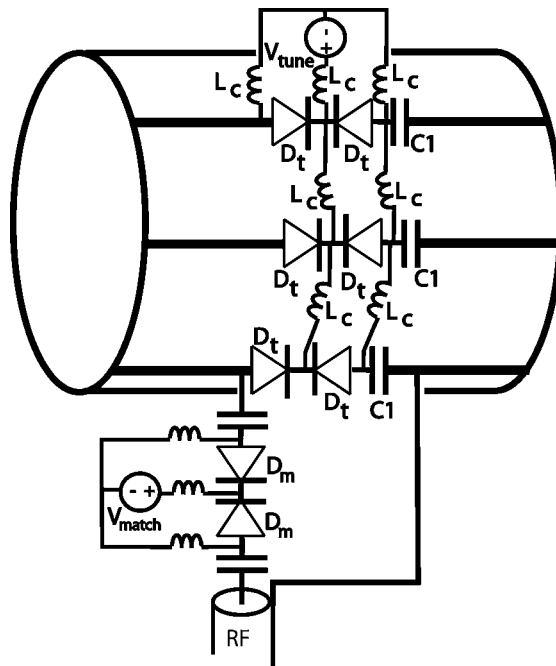


FIG. 1. The schematic diagram of the proposed autotune MRI RF coil. D_t are the tuning variable capacitor diodes (varactor) and D_m is the impedance matching varactor. L_c are the RF choke inductors.

the coil, all varactor diodes for tuning were connected in parallel with the bias source, therefore applying the same bias voltage to all of them. Capacitive coupling was used to drive the coil and a pair of varactor diodes were also used in the matching circuit, whose bias voltage could be adjusted separately to match the impedance of the birdcage coil resonator to 50 Ω line impedance. To reduce the RF signal coupling between these varactor diodes and also to isolate the coil from the DC bias voltage source, 2 μH axial RF choke inductors were used as shown in Fig. 1. We used isolation amplifiers (Analog Devices AD202) between the computer and the RF coil on the DC bias line to avoid ground loops and also to avoid any improper grounding that could lead to unbalanced loading. Two PCF8591P 8-bit CMOS digital-to-analog (D/A) converter devices (Philips Semiconductor) were used to generate the required bias voltages. The data were fed to the serial I²C-bus interface of the D/A circuits through the parallel port of an IBM PC-compatible Pentium computer (see Fig. 2).

A code was written using LABVIEW to communicate with the HP 4395A network analyzer (equipped with s-parameter test set) and the PCF8591P D/A circuits. The user inputs the required operating frequency to the PC and the software adjusts the reverse bias voltages of the varactor diodes on the legs iteratively to tune the coil at the desired operating frequency. After each DC voltage increment or decrement on the tuning diodes, the computer monitors the scattering parameter S11 within a 20-MHz bandwidth via the network analyzer. By reading the frequency of the minimum of S11 within this bandwidth, the software calculates the required voltage increment or decrement size. This is

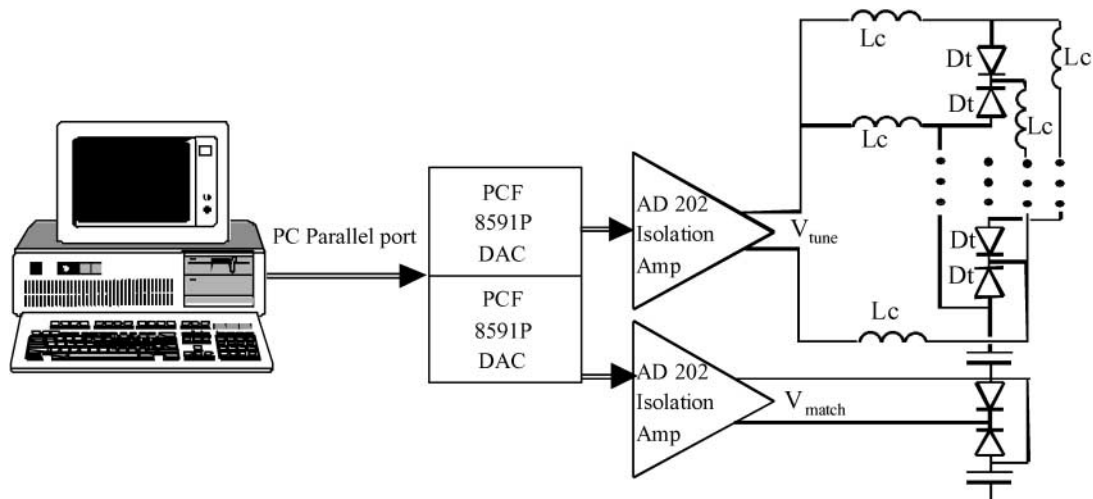


FIG. 2. The circuit diagram of the varactor bias voltage controller circuit. The PC controls the D/A card through the parallel port. The full coil circuit and the fixed capacitors on the legs of the coil are not shown.

done by using the heuristically found relation $\Delta V_1 = 0.15 \times \Delta f$. Here, ΔV_1 is the voltage increment/decrement amount and Δf is the difference between the observed tuning frequency and the target frequency. This allows faster convergence by taking large steps when far from the target frequency and smaller steps when near it to achieve an accurate tuning. Once the coil is tuned to the target frequency, the matching capacitance is adjusted to obtain 50Ω impedance at the coil input. This algorithm tries to minimize the S11 within the range of the matching capacitor. This matching procedure shifts the resonance of the coil slightly, so a final iteration on tuning is done to tune and match the coil at the exact resonance frequency.

A prototype of the automatically tuned multinuclear imaging coil was implemented and tested with a multicompartmental phantom filled with CuSO_4 and hexafluorobenzene (C_6F_6) solutions. Two small tubes of CuSO_4 solution and two small tubes of C_6F_6 were placed diagonally inside a larger cylinder with 45 mm inner diameter and 55 mm height. The inner diameter of the small tubes was 12 mm. This phantom is placed inside the coil with the axis of the cylinders placed vertically. A schematic of the phantom is shown in Fig. 3.

Images were acquired using a 3-T whole-body magnet (MagneX Scientific) interfaced with a console from SMIS (formerly known as Surrey Medical Imaging Systems, now Magnetic Resonance Research Systems, Surrey, U.K.). During the experiment, at first the coil was tuned automatically to 127.86 MHz and a proton image was acquired. After that, the operating frequency of the coil and the MR scanner were changed to 120.298 MHz for fluorine imaging and a second image was collected. Images were acquired using a 2D spoiled gradient echo pulse sequence with six 5-mm-thick slices, 14 cm FOV, and $\text{TR/TE} = 800/5$ ms. Flip angle was 90° and the acquisition matrix size was 128×128 . Both images were acquired with 4 NEX to further improve the SNR. Images were interpolated to 256×256 during reconstruction by zero filling.

We also acquired the proton image of the same phantom using a passively tuned animal coil to compare the SNR of the proposed design. This coil was also built in-house and it has the same size as the autotuned coil. It is also an 8-leg low-pass coil which has fixed capacitor tuning for single-frequency operation at the proton resonance. Unlike the autotuned coil, this coil is fed in quadrature, which increases the obtained SNR by roughly $\sqrt{2}$. This factor is taken into account in SNR comparison. Using the same pulse sequence, a H-1 image of the phantom is acquired.

Finally, we did a test with the autotuned coil to observe the power level at which diodes go into Zener breakdown. In this test, we increased the peak amplitude of the RF pulse of a gradient echo sequence and observed the peak amplitude of the Fourier transform of the FID signal. The peak RF pulse amplitude was

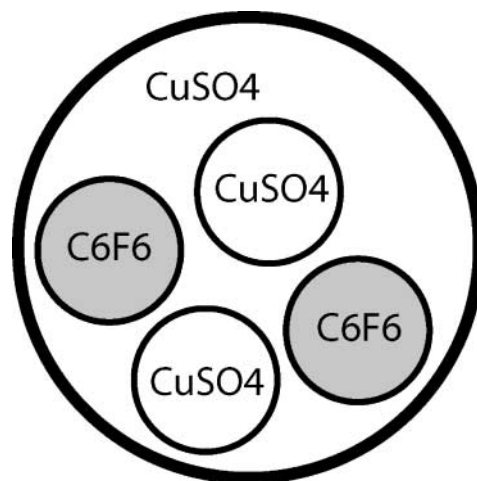
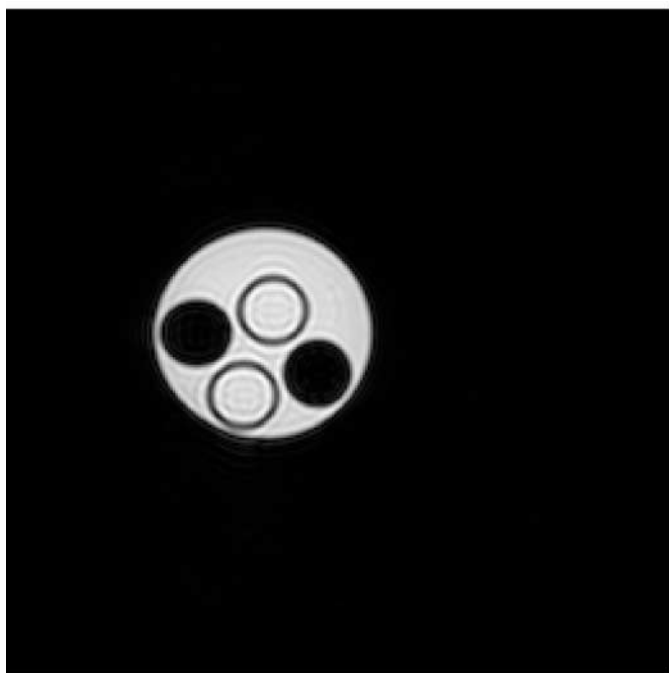
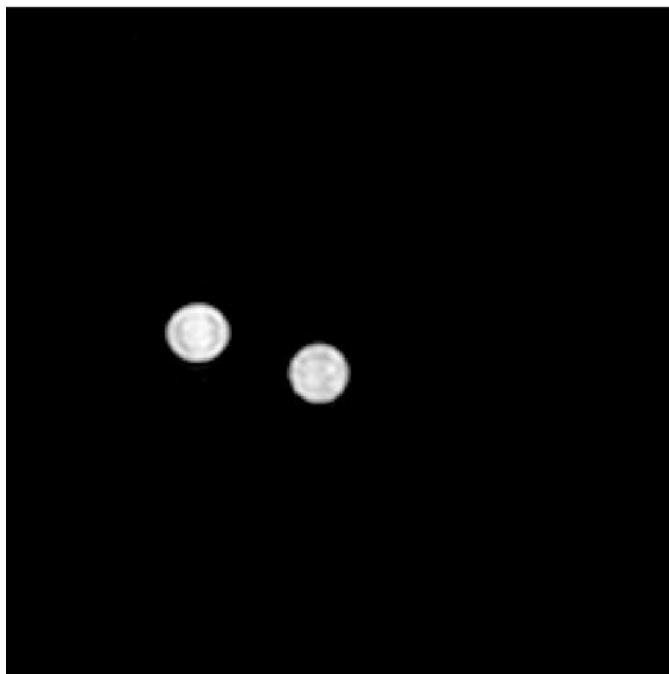


FIG. 3. Schematic diagram of the multicompartmental phantom filled with CuSO_4 solution and C_6F_6 . (Not drawn to scale).



(a)



(b)

FIG. 4. The images acquired at the operating frequency of (a) 127.86 MHz (CuSO_4 solution) and (b) 120.298 MHz (fluorine sample). A gradient echo pulse sequence was used to acquire the images. FOV was 140 mm with a slice thickness of 5 mm. Acquisition matrix was 128×128 . A TR/TE combination of 800/5 ms was used.

increased from 11 V (1.2 W peak power at 50Ω) to 87 V (76 W peak power at 50Ω) in approximately 5.5-V increments. The 90° flip angle is observed at 19 W peak instantaneous power.

RESULTS

Figure 4a shows the proton image that was acquired at the operating frequency of 127.86 MHz. As seen in the figure, only the tubes and the external cylinder filled with CuSO_4 solution could be observed, whereas tubes containing C_6F_6 showed up as dark discs. Similarly, Fig. 4b shows the F-19 image that was acquired at the operating frequency of 120.298 MHz. This time, only the tubes filled with the fluorine sample C_6F_6 were observed.

The SNR of each image was calculated by dividing the mean signal intensity in a selected ROI by the noise in the background. The noise in the background was calculated by multiplying the measured standard deviation in the background by 1.4 to account for the rectified signal due to the magnitude operation. Using this method, the SNR of the F-19 image was found to be 65 and that of H-1 was 217. The SNR of the image acquired using the fixed capacitor phantom is calculated to be 295. When $\sqrt{2}$ factor obtained by the quadrature detection is taken into account, this can be compared to an SNR of 209 for a linearly fed coil.

The results of flip angle versus input power experiment were illustrated in Fig. 5. From this graph, it can be observed that the relation between applied power versus flip angle is almost linear up to a certain power level, as expected. However, above 50 W, a saturation is observed, an indication that the diodes probably start to conduct, clipping the peak of the applied RF pulse. The minimum reverse breakdown voltage of the diodes is given as 30 V in data sheets.

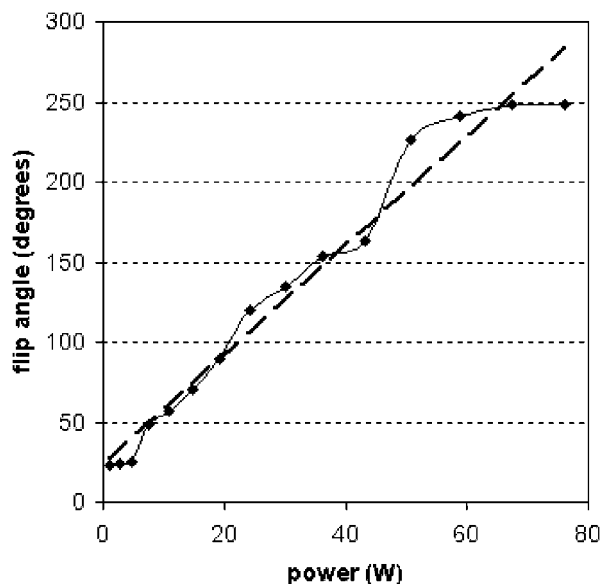


FIG. 5. Flip angle versus applied input power is illustrated. The dashed line shows the best linear fit for the data given. Saturation is observed above 50 W.

We also measured the time it took to change the operating frequency from one nucleus to the other. The tuning and matching was changed from proton to fluorine frequency in 39 s, whereas it took 67 s to go the other way.

DISCUSSION

In this study, we demonstrated the feasibility of an electronically controlled variable tuning RF coil for multinuclear imaging. We obtained very good tuning and matching ($S_{11} < -35$ dB) with a high loaded Q value ($Q_{\text{loaded}} \sim 300$ with the phantom covering roughly 6% of the coil volume) at both resonance frequencies. The Q_{loaded} was a little higher than normal owing to the fact that the filling factor was small and we did not add NaCl to the solution.

SNR is an important issue especially for imaging nuclei other than hydrogen. Since the concentration of these nuclei are much less than hydrogen in biological tissues as well as yielding MRI signals with smaller amplitudes relative to hydrogen (depending on the gyromagnetic ratio and the spin quantum number), one requires the best achievable SNR to obtain a good quality image. Therefore, good tuning and matching is an important factor to maximize the SNR.

It is a well-known fact that the tuning and matching of an MRI RF coil varies with different loads. In the present study, we obtained good matching and tuning for each individual load with a computer controlled variable tuning method. As one goes to higher field strengths, the separation between the resonance peaks of different nuclei will increase and hence coil perturbation methods will not be feasible. In this study, we used the designed coil for imaging two nuclei; however, it is possible to obtain good tuning and matching for any number of nuclei of interest even at high field strengths. The only restriction would be the sweep range of the varactor diodes. By choosing the appropriate diode, the sweep range can be designed to cover all the frequencies of interest.

To compare the SNR performance of the proposed coil, we also acquired images from the same phantom using a passively tuned birdcage coil. This coil was previously built in-house for animal imaging. Since this coil was constructed for quadrature operation, direct SNR comparison was not possible. On the other hand, when the $\sqrt{2}$ factor was taken into account, SNRs were comparable. By this comparison, the autotuned coil had 3.8% better SNR. However, one must also take into account that the theoretical $\sqrt{2}$ factor is not practically achievable. Due to slight mismatches in the quadrature channels and losses in the quadrature splitter/combiner, generally the gain in SNR is slightly lower than the theoretical expectations. On the other hand, these experiments demonstrate that the autotuned coil has SNR performance, comparable to fixed-tuning coils.

It should also be noted that neither the pulse sequence parameters nor the CuSO_4 concentration were optimized for best achievable SNR. Moreover, small filling factor (5.7% by volume), a wideband (10–200 MHz) receiver preamplifier (Miteq

AU-1466) with a noise figure of 1.1 at 100 MHz might have resulted in SNR values which are lower than expected. Optimized imaging parameters and a receiver with narrowband preamplifier, having a much lower noise figure, would improve the SNR values further.

In designing the proposed type of coil, one must be careful about the reverse breakdown voltage of the varactors. As we have shown in Fig. 5, the coil operates sufficiently linearly within the power levels required for this coil size. However, to achieve 90° and 180° flip angles with shorter RF pulse durations, the peak of the applied RF must be increased. This might cause the voltage on some diodes to exceed the breakdown voltage, resulting in unwanted distortions in slice profile. Besides, it will not be possible to achieve the required flip angles. Voltage division on series components will help avoid this problem to some extent, but it will not eliminate it. The same considerations would apply for larger coils where the required input power would be larger. This problem can be eliminated by using the proposed autotuned coil in receive-only mode, where the power to flip the spins will be supplied by a larger fixed-tuned coil and the signal will be received by the autotuned coil. Coil decoupling can be easily provided by disabling the bias voltage during RF gating pulses. This will enhance the SNR of the images but avoid diode Zener breakdown.

In the present work, we implemented a linear coil to simplify the design of the prototype. However, the idea can easily be adapted to quadrature-fed coils. Since the perturbation in the individual branches will be minimum, we expect that the isolation between the quadrature channels will be high, so that once the tuning is achieved, matching on the quadrature channels can be done independently.

The proposed coil can be used for sequential imaging of two or more different nuclei within a sample. However, in contrast to the double-resonance probes, it is not possible to use this design for applications such as decoupling that require simultaneous excitation of the two nuclei. But, if the voltage values required to tune the coil to different resonance frequencies are recorded before the beginning of an experiment, the controller computer can be synchronized with the scanner to switch between the two resonance frequencies, which will allow applications such as decoupling.

In the present study we used an expensive network analyzer, which was available in our lab, to demonstrate the feasibility and efficiency of such a design. However, it is possible to get the coil tuning and matching information with a simple circuit having a voltage-controlled oscillator, a directional coupler, and an amplitude detector. Our next goal is to develop this additional circuit and use the coil for high-resolution and multinuclear spectroscopic imaging of small animals.

ACKNOWLEDGMENT

This research was supported in part by PHS Grant P20 CA86182 awarded by the National Cancer Institute and the Cancer Research Program of the Chao Family Comprehensive Cancer Center at UC Irvine.

REFERENCES

1. J. Jin, G. Shen, and T. Perkins, On the field inhomogeneity of a birdcage coil, *Magn. Reson. Med.* **32**, 418–422 (1994).
2. P. M. Joseph and D. Lu, A technique for double-resonant operation of birdcage imaging coils, *IEEE Trans. Med. Imaging* **8**, 286–294 (1989).
3. J. Tropp, The theory of an arbitrarily perturbed bird-cage resonator, and a simple method for restoring it to full symmetry, *J. Magn. Reson.* **95**, 235–243 (1991).
4. A. Rath, Design and performance of a double tuned bird-cage coil, *J. Magn. Reson.* **86**, 488–495 (1990).
5. F. D. Doty, G. Entzminger, Jr., C. D. Hauck, and J. P. Staab, Practical aspects of birdcage coils, *J. Magn. Reson.* **138**, 144–154 (1999).
6. J. T. Vaughan, H. P. Hetherington, J. O. Otu, J. W. Pan, and G. M. Pohost, High frequency volume coils for clinical NMR imaging and spectroscopy, *Magn. Reson. Med.* **32**, 206–218 (1994).
7. J. P. Ledden, L. L. Wald, and J. T. Vaughan, A four port drive flat element transmission line coil for brain imaging at 3T, in “Proceedings of the 8th Scientific Meeting of the ISMRM, Denver, CO, 2000,” p. 1395.
8. J. S. Hyde, R. J. Rilling, A. Jesmanowicz, and B. Kneeland, Piezoelectric-controlled tuning capacitor for surface coils, *Magn. Reson. Med.* **12**, 50–55 (1989).
9. J. Rousseau, P. Lecouffe, and X. Marchandise, A new, fully versatile surface coil for MRI, *Magn. Reson. Imaging* **8**, 517–523 (1990).
10. F. Hwang and D. I. Hoult, Automatic probe tuning and matching, *Magn. Reson. Med.* **39**, 214–222 (1998).